Regenerative Therapy 25 (2024) 68–76

Contents lists available at ScienceDirect

Regenerative Therapy

journal homepage: http://www.elsevier.com/locate/reth

Original Article

Enhanced axon outgrowth of spinal motor neurons in co-culturing with dorsal root ganglions antagonizes the growth inhibitory environment

Zi-Xing Xu [a, b, c, *], Dan Xu [d], Fang Fang [e], Ying-Juan Fan [e], Bing Wu [f], Yu-Fan Chen [a], Hao-En Huang [a], Xin-Hao Huang [a], Yue-Hong Zhuang [d, **], Wei-Hong Xu [a, b, c, ***]

[a] Department of Spinal Surgery, The First Affiliated Hospital of Fujian Medical University, Fuzhou, Fujian Province, China
[b] Department of Orthopedics, National Regional Medical Center, Binhai Campus of the First Affiliated Hospital, Fujian Medical University, Fuzhou, Fujian Province, China
[c] Fujian Provincial Institute of Orthopedics, Fuzhou, Fujian Province, China
[d] Fujian Key Laboratory of Brain Aging and Neurodegenerative Diseases, Fujian Medical University, Fuzhou, Fujian Province, China
[e] Department of Pharmacology, Fujian Medical University, Fuzhou, Fujian Province, China
[f] The Central Laboratory, The First Affiliated Hospital of Fujian Medical University, Fuzhou, Fujian Province, China

ARTICLE INFO

Article history:
Received 23 September 2023
Received in revised form
9 November 2023
Accepted 22 November 2023

Keywords:
Central nervous system regeneration
Spinal motor neuron aggregates
Dorsal root ganglia transplantation
Experimental modeling
Axonal bridging
3D printing
Spinal cord injury

ABSTRACT

Introduction: Forming a bridge made of functional axons to span the lesion is essential to reconstruct the motor circuitry following spinal cord injury (SCI). Dorsal root ganglion (DRG) axons are robust in axon growth and have been proved to facilitate the growth of cortical neurons in a process of axon-facilitated axon regeneration. However, whether DRG transplantation affects the axon outgrowth of spinal motor neurons (SMNs) that play crucial roles in motor circuitry remains unclear.
Methods: We investigated the axonal growth patterns of co-cultured DRGs and SMN aggregates (SMNAs) taking advantage of a well-designed 3D-printed in vitro system. Chondroitin sulphate proteoglycans (CSPG) induced inhibitory matrix was introduced to imitate the inhibitory environment following SCI. Axonal lengths of DRG, SMNA or DRG & SMNA cultured on the permissive or CSPG induced inhibitory matrix were measured and compared.
Results: Our results indicated that under the guidance of full axonal connection generated from two opposing populations of DRGs, SMNA axons were growth-enhanced and elongated along the DRG axon bridge to distances that they could not otherwise reach. Quantitatively, the co-culture increased the SMNA axonal length by 32.1 %. Moreover, the CSPG matrix reduced the axonal length of DRGs and SMNAs by 46.2 % and 17.7 %, respectively. This inhibitory effect was antagonized by the co-culture of DRGs and SMNAs. Especially for SMNAs, they extended the axons across the CSPG-coating matrix, reached the lengths close to those of SMNAs cultured on the permissive matrix alone.
Conclusions: This study deepens our understanding of axon-facilitated reconstruction of the motor circuitry. Moreover, the results support SCI treatment utilizing the enhanced outgrowth of axons to restore functional connectivity in SCI patients.

* Corresponding author. Department of Spinal Surgery, The First Affiliated Hospital of Fujian Medical University, No. 20, Chazhong Road, Taijiang District, Fuzhou 350005, Fujian Province, China.
** Corresponding author. Fujian Key Laboratory of Brain Aging and Neurodegenerative Diseases, Fujian Medical University, No. 1, Xue Yuan Road, Minhou County, Fuzhou 350122, Fujian Province, China.
*** Corresponding author. Department of Spinal Surgery, The First Affiliated Hospital of Fujian Medical University, No. 20, Chazhong Road, Taijiang District, Fuzhou 350005, Fujian Province, China.
E-mail addresses: xuzixing@fjmu.edu.cn (Z.-X. Xu), zhuangyuehong@163.com (Y.-H. Zhuang), xuweihongfj@163.com (W.-H. Xu).
Peer review under responsibility of the Japanese Society for Regenerative Medicine.

https://doi.org/10.1016/j.reth.2023.11.013

1. Introduction

Globally, there were estimated 6.2 million people living with disability of spinal cord injury (SCI) in 2019 [1]. Traumatic SCI leads to disruptions in the neural circuitry and results in refractory para- or tetraplegia. Due to the limited capacity for self-repair in central nervous system (CNS) neurons, patients with complete injuries have a low chance to gain functional recovery. In the last decades, replacement therapy based on stem cells (SCs) transplantation has been shown to be capable of repairing the neural circuitry due to its potential effect on connecting the injured proximal and distal ends by differentiating into neurons [2,3].

In spite of the progress in cells transplantation, it still faces the difficulty in long distance of axonal elongation, glial scar barrier and local inhibitory environment, which ought to be carefully considered before the goal of functional connectivity can be achieved [4]. Numerous efforts have been undertaken to date targeting the myelin associated inhibitors (MAIs) and receptors [4–6], inhibitory components of the glial scar (e.g. chondroitin sulphate proteoglycans, CSPG) [7,8], as well as pathological conditions (excitotoxicity, lipid peroxidation, inflammation and edema, etc.) [9,10]. Furthermore, promoting neuromodulation (brain/spinal cord stimulation strategies and brain-machine interfaces) [11], screening and optimizing the candidates of cells and grafts [12,13] have also been extensively investigated.

So far, SCs including mesenchymal stem cells (MSCs), induced pluripotent stem cells (iPSCs), and embryonic neural stem cells (eNSCs) have shown the ability to differentiate into neurons and replace the damaged neural tissue [3,14,15]. However, the adverse effects, such as immune rejection and tumorigenicity, are still of major concerns. Neural cells derived from central or peripheral nervous system such as schwann cells [16], olfactory ensheathing cells (OECs) [17] and dorsal root ganglion (DRG) neurons [18,19] have also been applied as candidates to reconstruct neural circuits. DRG neurons served as a donor for SCI repair has not been fully investigated. In our previous work, axons generated from DRG neurons were robust in growth and have been proved to facilitate the growth of cortical neurons (CNs) in a process of axon-facilitated axon regeneration [20]. Further, DRG axons were mechanically stretched and encapsulated in a collagen hydrogen to repair a SCI model in rats with a 5 mm complete transection at the thoracic level. The stretch-grown DRG axons in engineered grafts were found to overcome the obstacle by penetrating into glial scar tissue [21]. Overall, DRG neurons might be a favorable candidate for SCI treatment.

Since there is still a lack of data showing whether DRG transplantation affect the axon outgrowth of spinal motor neurons (SMNs) that play crucial roles in motor circuitry, based on preceding works, we hypothesize that axon outgrowth of SMNs can be enhanced and guided by the extension of DRG axons; moreover, co-culture of SMNs and DRGs is capable of overcoming the inhibitory environment containing CSPG after SCI. Therefore, SMN axons were studied by co-culturing with DRGs in a three-dimensional (3D) printed co-culture system in the present work.

2. Materials and methods

2.1. Preparation of co-culture system by 3D printing technique

The co-culture system was designed for investigating the relationship of axonal growth between DRGs and SMNs. The process consists of three steps: (1) Preparation of 3D printed negative molds; (2) Polydimethylsiloxane (PDMS) casting with the molds in a 6-well plate to form culture chambers; and (3) Preparation of 3D printed channel/baffle plates matched with the chambers. Briefly, negative molds used for casting culture chambers were designed in AUTODESK 123D Design software (Version2.2.14). Then the data was imported into Print 3D software (Version3.3.791.0) in controlling of the 3D printer (FORTUS 450mc, Stratasys, USA) to perform the printing process. The printed molds were then placed into a 6-well plate and perfused with PDMS mixed alcohol. Next, the plate was transferred into a vacuum pump and vacuumized for 2 h. Followed by drying and curing at 50 °C for 8 h, molds were removed and PDMS culture chambers were harvested. The preparation of the channel or baffle plates was similar to that of culture chambers with slight difference in the step of removing the molds. Poly (ethylene terephthalateco-1,4-cylclohexylenedimethylene terephthalate) (PETG) and Polyvinyl alcohol (PVA) were used for culture chambers and channel/baffle plates printing, respectively. PVA is water-soluble and removed after soaking with distilled water for 1 h. PDMS mixed alcohol was prepared at a ratio of 1:10 (curing agent to PDMS). The printing parameters were listed in Table 1.

2.2. Isolation and culture of rat DRGs

All animal procedures in the study were carried out following the guidelines for the Welfare and Use of Laboratory Animals and approved by the Laboratory Animal Welfare & Ethics Committee of Fujian Medical University. DRGs obtained from the spinal cords of day-15 rat embryos (Fujian Medical University) were isolated as described elsewhere [22]. DRGs were cultured in Basic Medium (BM), which was formulated using Neurobasal medium supplemented with B-27 (2 %, Sigma–Aldrich), L-glutamine (0.4 mM, Invitrogen), glucose (2.5 mg/mL, Sigma–Aldrich), 2.5S nerve growth factor (10 ng/mL, NGF, Gibco) and fetal bovine serum (1 %, FBS, HyClone). Cytosine 1-β-D-arabinofuranoside (5 μM, Ara-C, Sigma–Aldrich), 5-fluoro-2′-deoxyuridine (5-FdU) (20 μM, Sigma–Aldrich) and uridine (20 μM, Sigma–Aldrich) were added into the BM in the first 2 days. Starting from day 3, BM containing 20 μM 5-FdU and 20 μM uridine was used for long-term culture.

2.3. Preparation of rat SMNs and SMN aggregates (SMNAs)

SMNs were prepared from day-14 embryonic rats as described by Graber et al. [23]. Briefly, the spinal cords were isolated from the embryonic rats, with dorsal root ganglia and meninges gently removed. Then, the spinal cords were placed in a 15-mL conical tube with 2 mL of trypsin solution for incubation in a 37 °C water bath for 3 min, followed by trituration in 0.02 % DNase to obtain cell suspension. Next, the cell suspension was layered in a 15-mL conical tube containing 2 mL of OptiPrep as a density gradient medium and the cells in the interface were collected, re-suspended in L-15 medium (Gibco), and plated on panning dishes which were previously coated with affinity-purified goat anti-mouse IgG in Tris-HCl buffer at 4 °C overnight. The cells then were washed and incubated with $p75^{NTR}$ antibody (Abcam ab6172, 1 μg/mL in PBS). After immunopanning, panning dishes were gently washed to remove those loosely attached cells. Adherent cells were collected

Table 1
Printing parameters.

Parameters	Values
Filament diameter (FDM, mm)	1.75
Printhead temperature (°C)	190–220
Printing platform temperature (°C)	70
Printhead movement speed (mm/s)	30
Needle inner diameter (mm)	0.3
Layer thickness (mm)	0.1

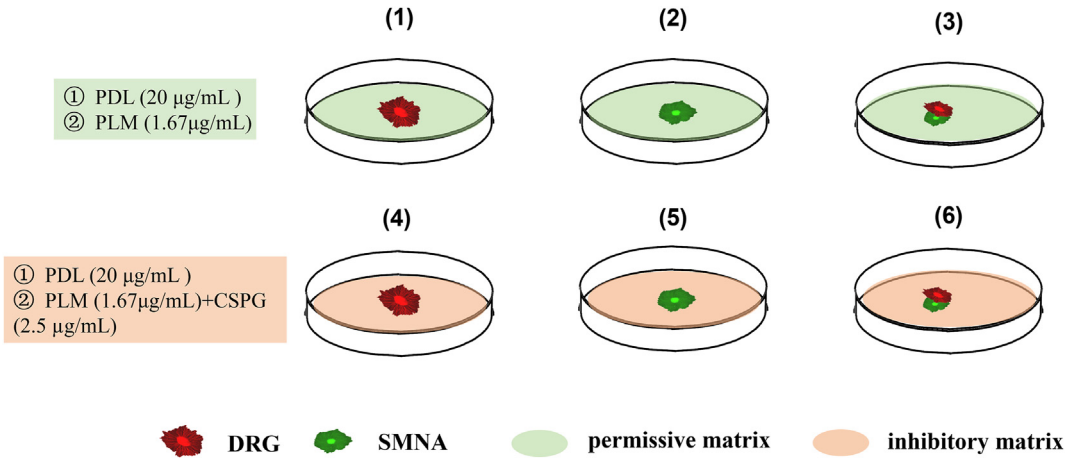

Fig. 1. Experimental groups for studying axon growth patterns of neuron aggregates cultured on the permissive or inhibitory matrix.

by trypsinization and centrifugation, then re-suspended by motor neuron growth medium supplemented with brain-derived neurotrophic factor (BDNF, 10 ng/mL in final concentration, the same below, Antigenix America), ciliary neurotrophic factor (CNTF, Peprotech 450-13) and glial cell line-derived neurotrophic factor (GDNF, Peprotech 450-10). An aliquot (10 μL) was used for counting.

SMN aggregates (SMNAs) were prepared as described previously [20]. The mold contains 9 square-based pyramids with a side length of 4.0 mm slanted at a 60° angle. These pyramids are arranged in a 3 × 3 array. The mold is used to create PDMS templates (with a ratio of 1:10 for the curing agent to PDMS) that can be placed into a 12-well plate, which could serve as a micro-well array that can force the formation of SMN aggregates by centrifugation. After obtainment of the PDMS templates, spinal motor neurons were diluted to 4.0 × 10^6 cells/mL, and 10 μL of suspension was added into each micro-well, and then centrifuged at 1200 g for 5 min to fling SMNAs towards the base of each micro-well. The plates were then cultured for 24 h at 37 °C in a humidified 5 % CO_2 incubator to promote neuronal adhesion and SMN aggregates formation.

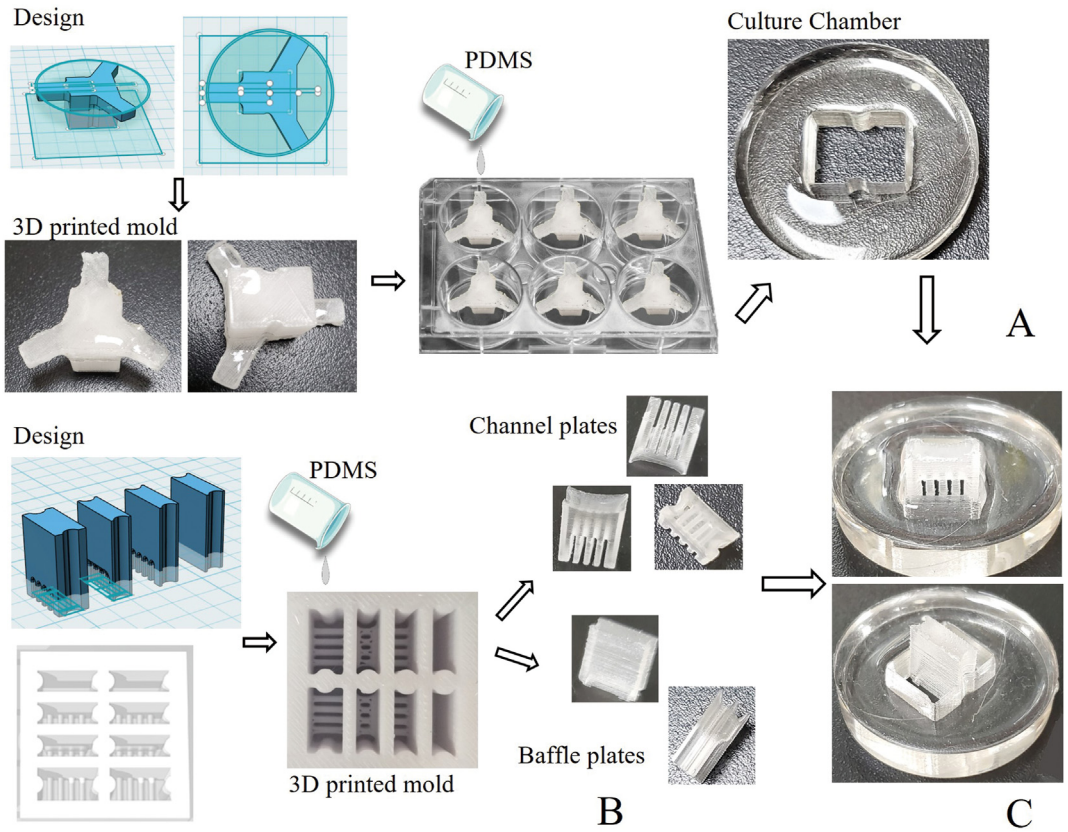

Fig. 2. Schematic diagram of the procedure for preparation of co-culture system. (A) Sketch the negative mold in AUTODESK 123D Design software and print with the 3D printer, followed by PDMS casting process in a 6-well plate to form the culture chamber. (B) Sketch the molds of channel and baffle plates in AUTODESK software and print with the 3D printer, followed by PDMS casting process to form the channel and baffle plates. (C) Assemble the culture chamber with channel/baffle plates to form co-culture system.

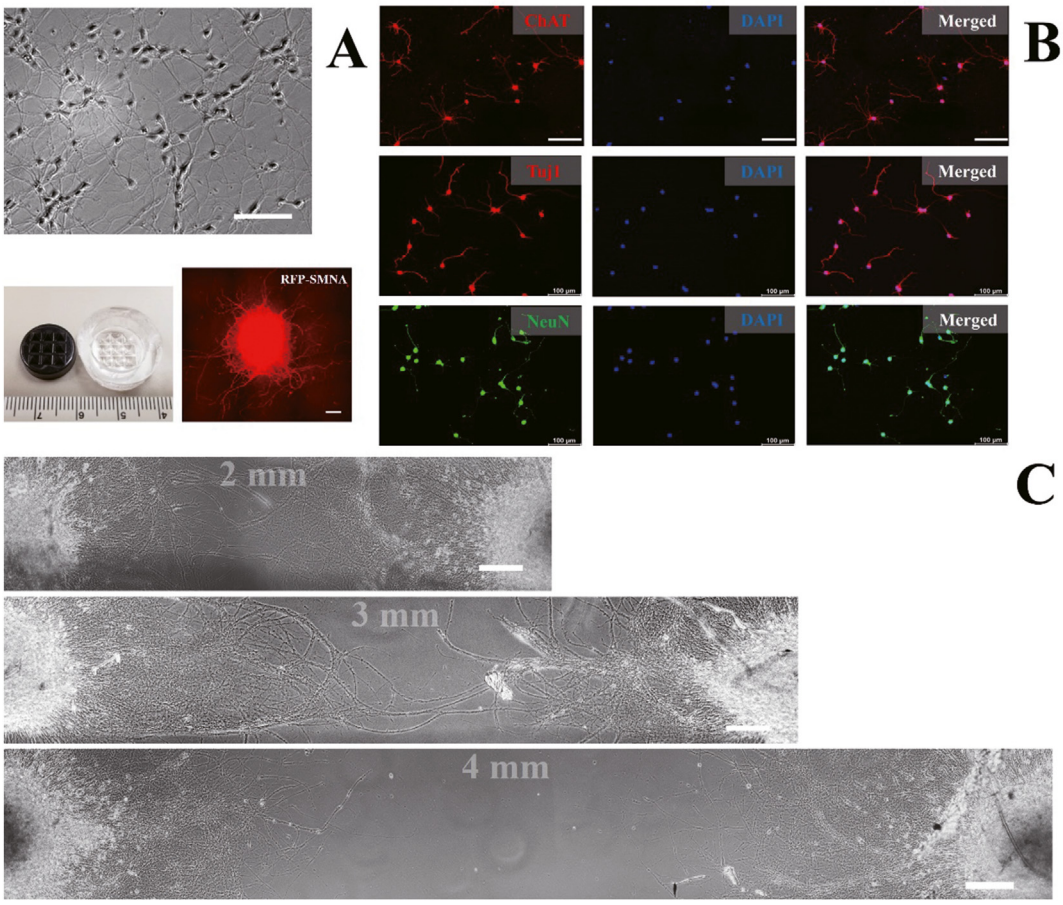

Fig. 3. A: The SMNs in dispersed culture on the 5th day (upper). 3D printed mold and PDMS template for SMNA preparation (lower left) and the RFP-transduced SMNA plated on the 3rd day (lower right). B: The cultured SMNs were immunofluorescently identified as positive for ChAT, Tuj1 and NeuN. C: Different degrees of axonal connections shown at two populations of SMNAs plated at various distances. Robust axonal connections formed in 2 mm of distance (upper), a small number of axonal connections formed in 3 mm of distance (middle) and no axonal connection was observed in 4 mm of distance (lower). Scale Bar: A, B: 100 μm C: 200 μm.

2.4. Co-culture of DRGs and SMNAs in vitro

Prior to the plating of DRGs, or SMNs, the culture surfaces were treated with 20 μg/mL poly-D-lysine (PDL, Sigma–Aldrich) for 2 h and rinsed with culture water (Lonza, Walkersville, MD) 3 times, and then treated again with 0.3 mL of 1.67 μg/mL human placental laminin solution (PLM, Sigma–Aldrich). In addition, neurons were transduced with enhanced green fluorescence protein (eGFP) or red fluorescent protein (RFP). Adeno-associated virus vectors (AAVs) including AAV1-hSyn-GFP (3.17×10^{13} genomic copies per milliliter) and AAV1-hSyn-tdTomato (2.28×10^{13} genomic copies per milliliter) that were used for transduction were provided by Vigene Bioscience (Jinan, China). The concentration of AAVs included in transduction medium was 1:2000 (V/V). After transduction for 24 h at 37 °C in a humidified 5 % CO_2 incubator, the transduction medium was entirely replaced with fresh medium.

With the aim of studying the growth relationship between DRG and SMNA axons in vitro, two populations of SMNAs were plated at a separating distance of 6 mm (a distance that SMNAs cannot achieve axonal connections spontaneously) in axonal growth channels, and transduced with RFP on the 3rd day. Twenty-four hours later, the medium with AAVs was replaced with fresh medium. On the 5th day, two populations of DRGs were plated outside the SMNAs on both sides, and the co-culture system was then transduced with eGFP and maintained up to 14 days for observation.

2.5. Co-culture of DRGs and SMNAs in CSPG induced inhibitory environment

To study how DRG axons affect the axon outgrowth of SMNs in CSPG environment, neurons in culture were divided into six groups: (1) DRGs cultured on the permissive matrix; (2) SMNAs cultured on the permissive matrix; (3) DRGs and SMNAs co-cultured on the permissive matrix; (4) DRGs cultured on the inhibitory matrix; (5) SMNAs cultured on the inhibitory matrix; (6) DRGs and SMNAs co-cultured on the inhibitory matrix (Fig. 1). The permissive matrix was prepared with PDL and PLM in sequence as above-mentioned. The inhibitory matrix was prepared with PDL followed by coating with PLM (1.67 μg/mL) and CSPG (2.5 μg/mL, CC117, Sigma–Aldrich) for 5 h and rinsing for 3 times. The cultures were maintained for 1, 3, 5 and 7 days for observation of axonal growth.

For distinguishing the axons extended from DRGs or SMNs in the co-culture system, neurons were transduced with RFP or eGFP respectively in advance, using the 3D printed culture chambers as well as baffle plates mentioned above. In general, it takes 4–5 days for the axons to exhibit distinguishable fluorescence under fluorescence microscope. After co-culturing for the specific time (5 or 7 days), the neurons and axons in the same field of view were photographed under both green (532 nm) and blue (488 nm) excitation wavelengths. Then, the axons extended from DRGs or SMNs exhibited red or green fluorescence respectively. The lengths of

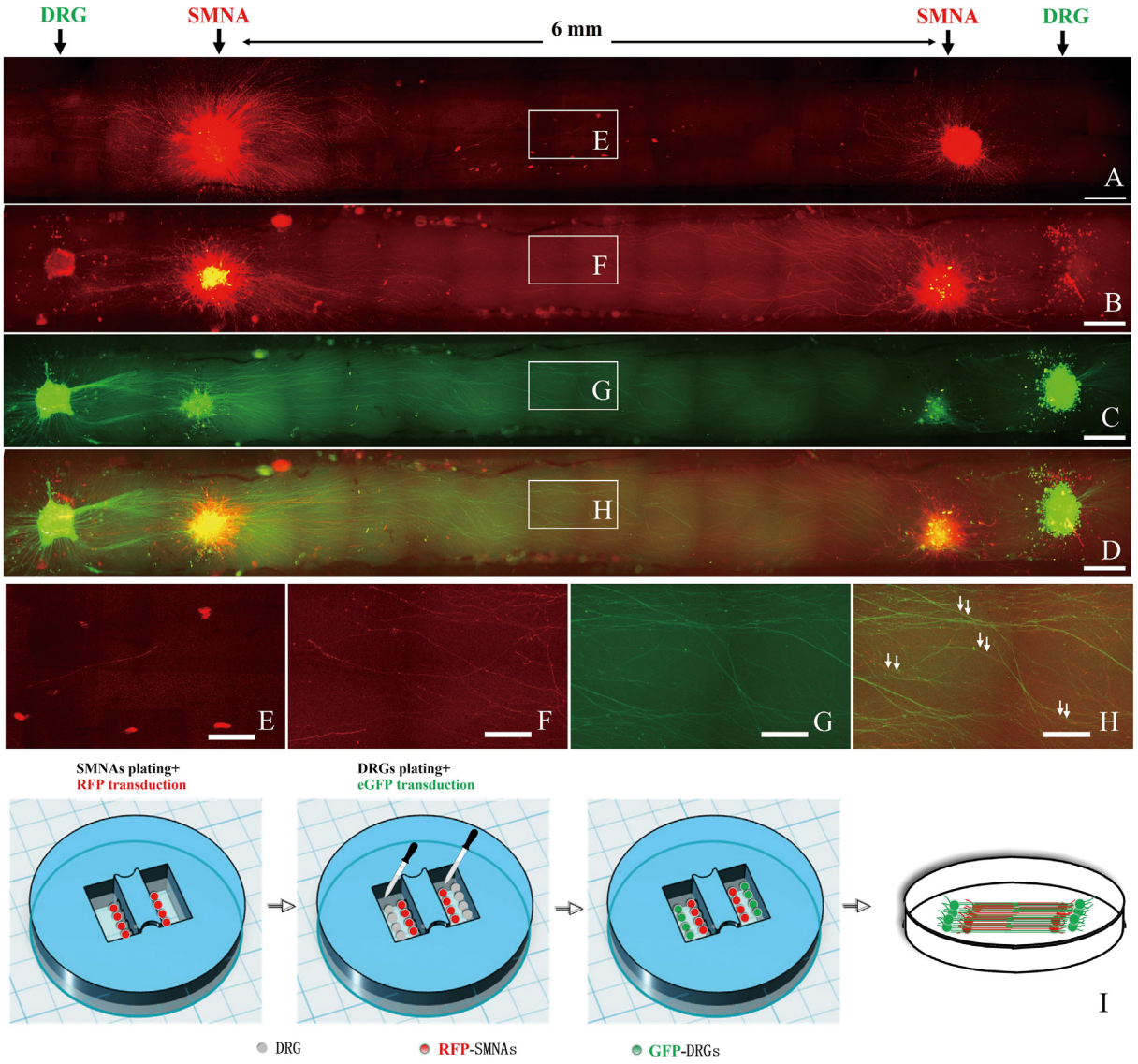

Fig. 4. Axonal guidance study on a co-culture system of DRGs and SMNAs. Two populations of SMNAs (transduced with RFP) were plated at a distance of 6 mm and DRGs (transduced with eGFP) were plated 5 days later on either side of the SMNAs (see sketch map in Fig. 4I). Without the guidance of DRG axons, no axonal connection was achieved in two populations of SMNAs plated at a distance of 6 mm (A). Comparatively, with the secondary plating of DRGs, SMNA axons extended to reach the opposing SMNAs (B) on account of the full connection of DRG axons generated from the both sides (C). A tag-merged view of the region between SMNAs shows a parallel growth relationship between DRG and SMNA axons (D). The magnified views of the regions in the center of A–D show the details of the axon outgrowth between two populations of SMNAs (E–H). White arrows indicate the parallel growth relationship between DRG and SMNA axons. Scale Bar: A–D: 300 μm; E–H: 100 μm.

axons were measurable individually by using NeuronJ plug-in for Fiji Image J (version 1.51n, National Institutes of Health, NIH, USA). For quantitative analysis, each neuron aggregate in specific group was prepared in triplicate. Ten random axons from each of neuron aggregate were chosen for measurement. Thus, a total of 30 counts in each group (n = 3 per group) were included for analysis.

2.6. Immunohistochemistry

Neurons were cultured on coverslips and fixed for 15 min at room temperature with 4 % paraformaldehyde. Afterwards, the cells were incubated in PBS containing 0.5 % Trtion X-100 for 15 min at room temperature to increase permeabilization, followed by incubation in 10 % goat serum for 30min. Then, the rabbit anti-ChAT antibody (Beyotime, AF6497, 1:500), mouse anti-neuron-specific Class III β-tubulin antibody (Tuj1, Covance, MMS-435P, 1:500), or rabbit anti-NeuN (Proteintech, 26975-1-AP, 1:500) was added to the cell slides for incubation overnight at 4 °C, followed by incubation for 30 min at 37 °C with Cy3-labelled goat anti-rabbit IgG (H & L) (Beyotime, A0516, 1:500), Cy3-labelled goat anti-mouse IgG (H & L) (Beyotime, A0521, 1:500) or Dylight 488-labelled Goat anti-rabbit IgG (H & L) (Abcam, ab96883, 1:1000) as the second antibody, respectively. Then, the coverslips were incubated with DAPI (Beyotime, C1005, 1:1000) for 10 min. At each step, slides rinsing with PBS for 5 min (×3) was performed. Finally, the coverslips were flipped onto a drop of mounting anti-fading media (Beyotime, P0126, 1:1000) placed on a slide. The motor neurons were photographed by a Confocal Microscope (LSM780, Zeiss, Germany).

2.7. Statistical analysis

Statistical analyses were conducted using SPSS 19.0 (SPSS Inc., Chicago, IL, USA). Experiment data were presented as mean ± standard deviation. One-way analysis of variance (ANOVA)

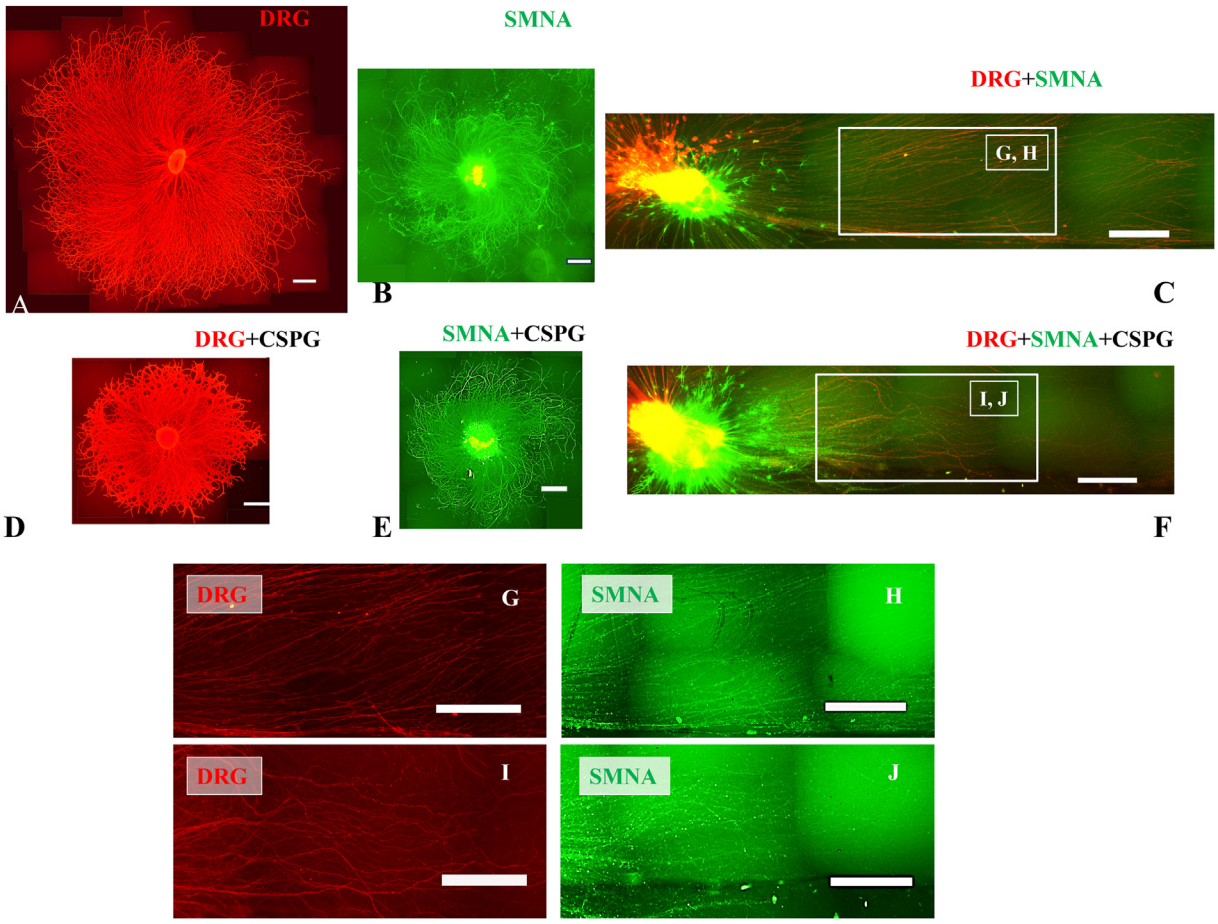

Fig. 5. Axon outgrowth on different matrixes. Compared to the neurons cultured on a permissive matrix in (A) (DRG) and (B) (SMNA), the axons in co-culture (the same matrix) exhibited more robustness in axonal elongation and an obvious pattern of parallel growth relationship (C). Comparatively, the neurons cultured on the CSPG induced inhibitory matrix showed the suppressed axon outgrowth of DRG (D) alone, SMNA (E) alone or in co-culture (F). The magnified views of the regions in C, F show the details of the DRG (red) (G, I) and SMNA (green) (H, J) axons on the permissive (G and H) or inhibitory (I and J) matrix. The parallel growth relationship between DRG and SMNA axons was observed.

with the Fisher LSD post-hoc test was used for multiple group comparisons. Dunnett's T3 test was performed when variances were unequal. A p value less than 0.05 was considered as statistically significant.

3. Results

3.1. Co-culture system for neurons in vitro

As shown in Fig. 2, the culture chamber produced by PDMS was 8 mm in depth, 11 mm in width and 14 mm in length, with a semicylindrical protrusion (2.0 mm of radius) in the center of each long side to match the channel or baffle plates. The channel plate divides the culture chamber into two connected wells capable of exchanging nutrients through the inner channels (each 1 mm in width). The axons generated from both sides of neurons were maintained and extended along the channels. The baffle plate divides the culture chamber into two independent wells to culture neurons separately, in case of co-culture is in demand, it could be removed or replaced by the channel plate. The width of the channel or baffle plate was adjustable to meet the requirement in culture. The distance of two populations of neurons plated was variable according to the width of the plate.

3.2. Separate cultures of SMNs, SMNAs and DRGs explants

Cultured SMNs/SMNAs adhered to the plate within 3 h and extended neurites at 24 h. Neuronal cell bodies and neurites in dispersion culture appeared to enlarge and elongate up to a number of outgrowing neurites capable of forming an interwoven network at 4–5 days following plating (Fig. 3A). The longest distance that two populations of SMNAs plated at a separating distance were capable of forming axonal connections was 3 mm (Fig. 3C). Different axonal connections because of the diverse distances of SMNAs plated were shown in Fig. 2C (observed on the 7th day). The cultured SMNs were immunofluorescently identified as positive for ChAT, Tuj1 and NeuN. The purity of ChAT positive neurons was calculated as (94 ± 2) % (Fig. 3B).

The culture of DRGs was consistent with our previously published work [20]. Briefly, DRG neurons adhered tightly to the plate and began to extend axons after 12 h of culture. Non-neuronal cells were eliminated with time without affecting neuronal viability because of the application of Ara-C during the first 48 h.

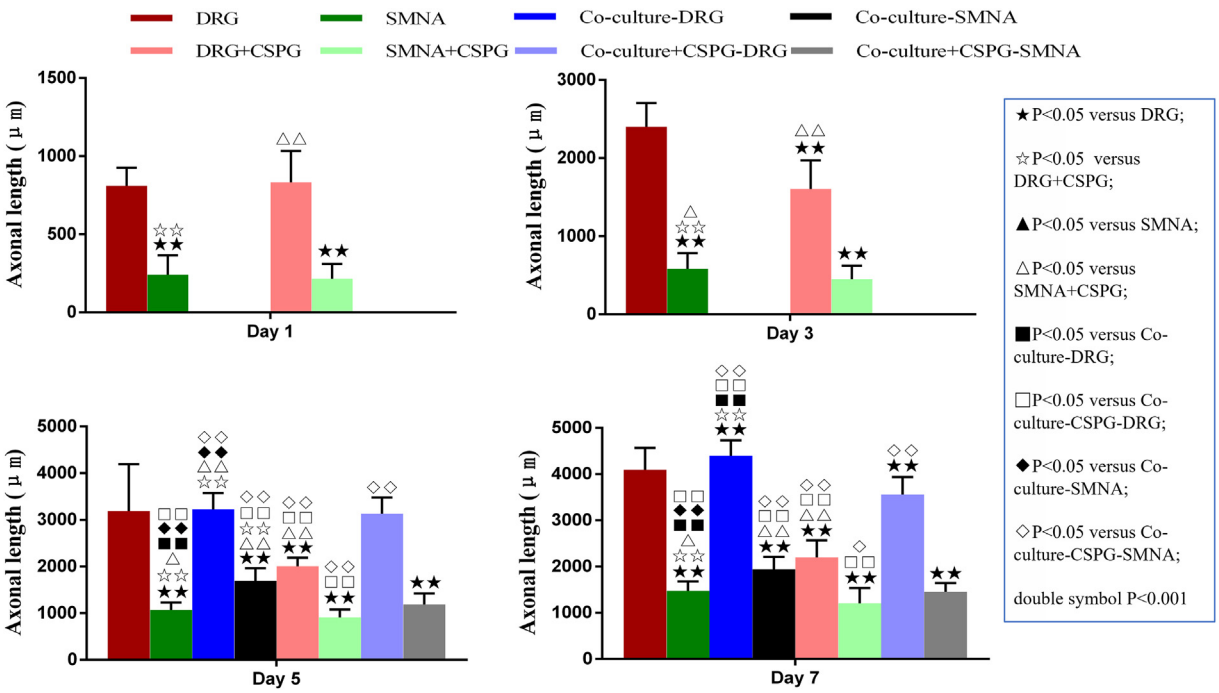

Fig. 6. The statistical comparisons among the different groups. Co-culture seemed to be antagonistic against the inhibitory environment, because the lengths of SMNA axons in co-culture on the CSPG-coating surface were not statistically different to that SMNAs cultured alone (P > 0.05). Scale Bar: A–J: 500 μm ★P < 0.05 versus DRG; ☆P < 0.05 versus DRG + CSPG; ▲P < 0.05 versus SMNA; △P < 0.05 versus SMNA + CSPG; ■P < 0.05 versus Co-culture-DRG; □P < 0.05 versus Co-culture-CSPG-DRG; ◆P < 0.05 versus Co-culture-SMNA; ◇P < 0.05 versus Co-culture-CSPG-SMNA; double symbol P < 0.001.

3.3. Axonal growth patterns of DRGs and SMNAs in the co-culture system

As the control, no axonal connection was seen in two populations of SMNAs plated at a separating distance of 6 mm (Fig. 4A, E). Relatively, five days after plating of SMNAs, DRG explants were plated on either side of the SMNAs and were observed to form axonal connections between two populations of SMNAs at day 14 (Fig. 4B–D, 4F–H). As the DRG axons extended beyond the SMNAs and formed connections with one another (green axons), a robust extension of the SMNA axons was observed. In addition, the SMNA axons appeared to be growing in parallel to the DRG axons (white arrows in Fig. 4H). The schematic drawing of the experiment was shown in Fig. 4I.

Table 2
Axonal length measured in different groups.

Group			Axonal length (μm)			
			Day 1	Day 3	Day 5	Day 7
(1)		Mean	810	2400	3190	4092
DRG		SD	117	303	1001	475
(2)		Mean	242	584	1070	1472
SMNA		SD	124	200	163	211
(3)	DRG	Mean	N/A	N/A	3226	4399
Co-culture		SD	N/A	N/A	350	332
	SMNA	Mean	N/A	N/A	1693	1945
		SD	N/A	N/A	272	267
(4)		Mean	833	1603	2006	2203
DRG + CSPG		SD	200	369	185	367
(5)		Mean	216	448	911	1212
SMNA + CSPG		SD	95	176	172	323
(6)	DRG	Mean	N/A	N/A	3139	3556
Co-culture + CSPG		SD	N/A	N/A	349	385
	SMNA	Mean	N/A	N/A	1184	1456
		SD	N/A	N/A	238	192
	F		215.633	363.695	318.528	444.512
	P		0.000	0.000	0.000	0.000

N/A: data not achievable before Day 5.

3.4. Axon outgrowth of DRGs & SMNAs in CSPG induced inhibitory environment

As controls, both of DRGs and SMNAs cultured on the permissive matrix extended the axons over time. DRGs exhibited more robust axonal elongation than SMNAs at all time points (P < 0.001). Compared to neurons cultured on a permissive matrix, CSPGs reduced the axonal length of DRGs and SMNAs by 46.2 % and 17.7 % (data shown on the 7th day, the same below), respectively. Due to the time window needed for the AAVs transduction mentioned above, the data in Group (3) and (6) was not achievable before Day 5. In the study, co-culture promoted the axon outgrowth of DRGs and SMNAs, although no statistical significance was found in DRGs. The increase rates were 7.5 % and 32.1 %, respectively. In contrast, CSPG limited the axonal elongation of DRGs and SMNAs in co-culture by 19.2 % and 25.1 %, respectively. Interestingly, co-culture seemed to be antagonistic against the inhibitory environment, because the lengths of SMNA axons in co-culture on CSPG-coating surface were similar to that SMNAs cultured alone without CSPG (P > 0.05). The quantitative data and statistical comparisons among the different groups were summarized in Figs. 5,6 and Table 2.

4. Discussion

In mammals, the corticospinal motor circuitry plays a crucial role in controlling skilled and complex coordinating movements that can be damaged by SCI [24,25]. Thus, the aim to achieve functional recovery after SCI is reconstruction of the fundamental motor circuitry consisting of the motor cortex, corticospinal tracts (CST), and synaptic connections directly or indirectly with

motoneurons [26,27]. Harnessing the neuroplasticity of spared motor circuitry represents a highly promising therapeutic target for SCI [26]. The lack of long-distance axonal generation of severed fibers in the adult CNS was widely known, however, we have verified that the outgrowth of cortical neuronal axons could be guided and enhanced by the co-cultured DRGs. Furthermore, in the present study, we demonstrate the robust axonal growth of SMNs and their antagonistic effects against the inhibitory matrix containing CSPG in co-culturing with DRGs.

The loss of motor function results from the disruption of signal transmission between the brain and distal neural host. Therefore, forming a bridge made of functional axons to span the injury and reconnecting the neural tissue above and below the lesion is a primary task to overcome the neural network disconnection [28]. The significance of long distance of axon outgrowth following SCI is not only bridging the lesion site, but also promoting the intrinsic axonal sprouting via axon-facilitated effects [18,29]. DRG axons have been proved to form robust axonal connections spontaneously up to a separating distance of 10 mm [20]. They facilitate and guide the axon outgrowth of CNs in a model of two separating populations of CN aggregates plated at a distance of 4 mm. This phenomenon has also been demonstrated in co-culturing with SMNAs in the present work, even though we have extended the distance up to 6 mm. Our results show that compared to the negative control without DRG bridges, the SMNAs plated with DRGs demonstrated enhanced outgrowth along the DRG axon bridge to distances that they could not otherwise reach. The promotion was quantitatively verified by the co-culture study showing that the SMNA axonal length was increased by 32.1 %. In this study, SMNs were isolated and cultured from rat embryonic spinal cords by an immunopanning protocol taking advantage of several distinct properties of rat motor neurons to isolate them from neighboring cells. High level expression of ChAT was observed in our isolated SMNs. ChAT is exclusively expressed in motoneurons in the ventral spinal cord [30]. In addition, the SMNs were also positive for mature neuronal markers NeuN and Tuj1.

Following SCI, the microenvironment containing significantly increased inhibitory molecules in the extracellular matrix (ECM) and myelin sheath which limits the plasticity and regeneration ability of axons [31]. The up-regulation of inhibitory molecules comprised of CSPGs is the result of hyperplasia of reactive astrocytes [32]. Although astrocyte proliferation reduces and repairs the SCI damage, it also obstructs the elongation of the regenerated axons because of the formation of glial scar [33]. The scar border is a physicochemical barrier composed of astrocytes, fibroblasts, and microglia secreting CSPGs, collogen, and the dense ECM [34]. In vitro studies revealed that CSPG largely exhibits a repulsive effect on axonal regeneration, and a signal from CSPG modulates the actin cytoskeleton of outgrowing neurites through the Rho/ROCK pathway [35–37]. In this work, the CSPG induced inhibitory environment reduced the axonal length of DRGs and SMNAs by 46.2 % and 17.7 %, respectively. However, the inhibitory effect was antagonized by the co-culture of DRGs and SMNAs. Especially for SMNAs, they extended the axons across the CSPG-coating matrix, reached the lengths close to those of SMNAs cultured on the permissive matrix alone.

Our study adopts the 3D printing technology with following advantages: (1) the distance between two populations of neuron aggregates is adjustable to meet the experiment design; (2) the process of the culture is simplified due to the individualized culture chamber; (3) the outgrowth of axons is restricted in the specific channels and the observation is easily achievable. There are also several drawbacks in the study that needs to be considered. First, the study is limited and focuses only on the in vitro relationship of DRG and SMNA axons. The in vitro study has difficulty in fully simulating the complex environment of an injured spinal cord. Second, the culture system doesn't involve astrocytes and microglia, although CSPG is introduced to imitate the inhibitory environment following SCI, there's still a lack of complete components (such as myelin-associated glycoprotein, Nogo, and semaphorin) of the glial scar. Third, the molecular mechanism of how the DRG axons affect the axonal growth patterns of SMNs is still unclear that remain to be investigated. To our knowledge, axon outgrowth is guided by growth cones which control the activity of actin-binding proteins (ABP) via intracellular signaling cascades. ABP emerged as critical regulators of axon growth and synaptic formation by controlling filamentous actin (F-actin) dynamics [38,39]. The promotion of axon elongation by co-culture is probably related to changes of expression in ABP (e.g., profilin and cofilin), which are regulated by RhoA and its downstream kinase, ROCK. This conjecture can be verified by using comparative transcriptomic analysis.

5. Conclusions

In the present study, we have verified the hypothesis that axon outgrowth of SMNs can be enhanced by the co-cultured DRG axons, and the co-culture facilitates the SMN axons to overcome the obstacles in CSPG induced inhibitory environment. A well-designed co-culture system was 3D-printed to test that hypothesis. This study deepens our understanding of axon-facilitated reconstruction of the motor circuitry. Moreover, the results support the SCI treatment utilizing the enhanced outgrowth of axons to restore functional connectivity in SCI patients.

Authors contributions

Zi-Xing Xu designed the main experiments and wrote the manuscript. Dan Xu, Fang Fang and Ying-Juan Fan performed the main experiments. Bing Wu provided the technological support for 3D printing. Yu-Fan Chen, Hao-En Huang and Xin-Hao Huang assisted the performance of 3D printing experiments and conducted the statistical analysis. Yue-Hong Zhuang provided the feedback on the manuscript. Wei-Hong Xu edited the manuscript and figures.

Funding

This work was supported by Natural Science Foundation of Fujian Province (No. 2020J01947, No. 2021J02035) and Fujian Provincial Health Technology Project (No. 2021CXA019).

Declaration of competing interest

The authors declare that they have no known competing financial interests or personal relationships that could have appeared to influence the work reported in this paper.

Acknowledgements

The authors would like to thank Center for Brain Injury & Repair, Department of Neurosurgery, University of Pennsylvania for technical support in this work.

References

[1] Ding W, Hu S, Wang P, Kang H, Peng R, Dong Y, et al. Spinal cord injury: the global incidence, prevalence, and disability from the global burden of disease study 2019. Spine 2022;47:1532–40.
[2] Zipser CM, Cragg JJ, Guest JD, Fehlings MG, Jutzeler CR, Anderson AJ, et al. Cell-based and stem-cell-based treatments for spinal cord injury: evidence from clinical trials. Lancet Neurol 2022;21:659–70.

[3] Assinck P, Duncan GJ, Hilton BJ, Plemel JR, Tetzlaff W. Cell transplantation therapy for spinal cord injury. Nat Neurosci 2017;20:637–47.
[4] Chen X, Li H. Neuronal reprogramming in treating spinal cord injury. Neural Regen Res 2022;17:1440–5.
[5] Saeed Y. Title: immunotherapy; a ground-breaking remedy for spinal cord injury with stumbling blocks: an overview. Front Pharmacol 2023;14:1110008.
[6] Zheng B, Tuszynski MH. Regulation of axonal regeneration after mammalian spinal cord injury. Nat Rev Mol Cell Biol 2023;24(6):396–413.
[7] Francos-Quijorna I, Sánchez-Petidier M, Burnside ER, Badea SR, Torres-Espin A, Marshall L, et al. Chondroitin sulfate proteoglycans prevent immune cell phenotypic conversion and inflammation resolution via TLR4 in rodent models of spinal cord injury. Nat Commun 2022;13:2933.
[8] Tran AP, Warren PM, Silver J. New insights into glial scar formation after spinal cord injury. Cell Tissue Res 2022;387:319–36.
[9] Hellenbrand DJ, Quinn CM, Piper ZJ, Morehouse CN, Fixel JA, Hanna AS. Inflammation after spinal cord injury: a review of the critical timeline of signaling cues and cellular infiltration. J Neuroinflammation 2021;18:284.
[10] Xia M, Zhang Q, Zhang Y, Li R, Zhao T, Chen L, et al. Growth differentiation factor 15 regulates oxidative stress-dependent ferroptosis post spinal cord injury by stabilizing the p62-Keap1-Nrf2 signaling pathway. Front Aging Neurosci 2022;14:905115.
[11] Hutson TH, Di Giovanni S. The translational landscape in spinal cord injury: focus on neuroplasticity and regeneration. Nat Rev Neurol 2019;15:732–45.
[12] Ribeiro B, Cruz B, de Sousa BM, Correia PD, David N, Rocha C, et al. Cell therapies for spinal cord injury: a review of the clinical trials and cell-type therapeutic potential. Brain: J Neurol 2023;146(7):2672–93.
[13] Liu X, Hao M, Chen Z, Zhang T, Huang J, Dai J, et al. 3D bioprinted neural tissue constructs for spinal cord injury repair. Biomaterials 2021;272:120771.
[14] Kim YH, Ha KY, Kim SI. Spinal cord injury and related clinical trials. Clin Orthop Surg 2017;9:1–9.
[15] Aboul-Soud MAM, Alzahrani AJ, Mahmoud A. Induced pluripotent stem cells (iPSCs)-Roles in regenerative therapies, disease modelling and drug screening. Cells 2021;10.
[16] Bunge MB, Wood PM. Realizing the maximum potential of Schwann cells to promote recovery from spinal cord injury. Handb Clin Neurol 2012;109:523–40.
[17] Gilmour AD, Reshamwala R, Wright AA, Ekberg JAK, St John JA. Optimizing olfactory ensheathing cell transplantation for spinal cord injury repair. J Neurotrauma 2020;37:817–29.
[18] Iwata A, Browne KD, Pfister BJ, Gruner JA, Smith DH. Long-term survival and outgrowth of mechanically engineered nervous tissue constructs implanted into spinal cord lesions. Tissue Eng 2006;12:101–10.
[19] Huang JH, Zager EL, Zhang J, Groff RF, Pfister BJ, Cohen AS, et al. Harvested human neurons engineered as live nervous tissue constructs: implications for transplantation. Laboratory investigation. J Neurosurg 2008;108:343–7.
[20] Xu ZX, Albayar A, Dolle JP, Hansel G, Bianchini J, Sullivan PZ, et al. Dorsal root ganglion axons facilitate and guide cortical neural outgrowth: in vitro modeling of spinal cord injury axonal regeneration. Restor Neurol Neurosci 2020;38:1–9.
[21] Sadik ME, Ozturk AK, Albayar A, Branche M, Sullivan PZ, Schlosser LO, et al. A strategy toward bridging a complete spinal cord lesion using stretch-grown axons. Tissue Eng 2020;26:623–35.
[22] Shekarabi M, Robinson JA, Burdo TH. Isolation and culture of dorsal root ganglia (DRG) from rodents. Methods Mol Biol (Clifton, NJ) 2021;2311:177–84.
[23] Graber DJ, Harris BT. Purification and culture of spinal motor neurons from rat embryos. Cold Spring Harb Protoc 2013;2013:319–26.
[24] Wang Y, Wu W, Wu X, Sun Y, Zhang YP, Deng LX, et al. Remodeling of lumbar motor circuitry remote to a thoracic spinal cord injury promotes locomotor recovery. Elife 2018;7.
[25] Martin JH. Neuroplasticity of spinal cord injury and repair. Handb Clin Neurol 2022;184:317–30.
[26] Kazim SF, Bowers CA, Cole CD, Varela S, Karimov Z, Martinez E, et al. Corticospinal motor circuit plasticity after spinal cord injury: harnessing neuroplasticity to improve functional outcomes. Mol Neurobiol 2021;58:5494–516.
[27] Brown AR, Martinez M. From cortex to cord: motor circuit plasticity after spinal cord injury. Neural Regen Res 2019;14:2054–62.
[28] Fouad K, Popovich PG, Kopp MA, Schwab JM. The neuroanatomical-functional paradox in spinal cord injury. Nat Rev Neurol 2021;17:53–62.
[29] Smith GM, Onifer SM. Construction of pathways to promote axon growth within the adult central nervous system. Brain Res Bull 2011;84:300–5.
[30] Hu BY, Zhang SC. Differentiation of spinal motor neurons from pluripotent human stem cells. Nat Protoc 2009;4:1295–304.
[31] Bhattacharyya S, Dinda A, Vishnubhatla S, Anwar MF, Jain S. A combinatorial approach to modulate microenvironment toward regeneration and repair after spinal cord injury in rats. Neurosci Lett 2021;741:135500.
[32] Emerson J, Delgado T, Girardi P, Johnson GV. Deletion of transglutaminase 2 from astrocytes significantly improves their ability to promote neurite outgrowth on an inhibitory matrix. Int J Mol Sci 2023;24(7):6058.
[33] Clifford T, Finkel Z, Rodriguez B, Joseph A, Cai L. Current advancements in spinal cord injury research-glial scar formation and neural regeneration. Cells 2023;12.
[34] Gong L, Gu Y, Han X, Luan C, Liu C, Wang X, et al. Spatiotemporal dynamics of the molecular expression pattern and intercellular interactions in the glial scar response to spinal cord injury. Neurosci Bull 2023;39:213–44.
[35] Galindo LT, Mundim M, Pinto AS, Chiarantin GMD, Almeida MES, Lamers ML, et al. Chondroitin sulfate impairs neural stem cell migration through ROCK activation. Mol Neurobiol 2018;55:3185–95.
[36] Gopalakrishnan SM, Teusch N, Imhof C, Bakker MH, Schurdak M, Burns DJ, et al. Role of Rho kinase pathway in chondroitin sulfate proteoglycan-mediated inhibition of neurite outgrowth in PC12 cells. J Neurosci Res 2008;86:2214–26.
[37] Chen X, Zhang L, Hua F, Zhuang Y, Liu H, Wang S. EphA4 obstructs spinal cord neuron regeneration by promoting excessive activation of astrocytes. Cell Mol Neurobiol 2022;42:1557–68.
[38] Schneider F, Metz I, Rust MB. Regulation of actin filament assembly and disassembly in growth cone motility and axon guidance. Brain Res Bull 2023;192:21–35.
[39] Leite SC, Pinto-Costa R, Sousa MM. Actin dynamics in the growth cone: a key player in axon regeneration. Curr Opin Neurobiol 2021;69:11–8.